The Seismic Performance of Tunnel-Form Buildings with a Non-Uniform in-Plan Mass Distribution

Vahid Mohsenian[1*], Ali Nikkhoo[2], Soheil Rostamkalaee[3], Abdolreza S.Moghadam[4], Farzad Hejazi[5*]

1and 3- Postgraduate Researcher, Department of Civil Engineering, University of Science and Culture, Tehran, Iran

2- Associate Professor, Department of Civil Engineering, University of Science and Culture, Tehran, Iran

4-Associate Professor, Structural Engineering Research Center, International Institute of Earthquake Engineering and Seismology, Tehran, Iran

5-Associate Professor, Department of Civil Engineering, University Putra Malaysia, Putra, Malaysia

Abstract: The specific operating conditions in concrete box-type (tunnel-form) buildings would lead to the concentration of walls in the interior parts of the plan and lack of structural walls in the perimeter of the plan. In this situation, due to the considerable reduction in torsional stiffness, usually torsional vibration modes prevail over translational vibration modes, therefore the building behaves as a torsionally flexible structure. Torsionally flexible buildings are often more sensitive to the eccentricities of mass and stiffness as well as the intensity of the torsional component of an earthquake, in which, an increase in these parameters results in both increased forces and displacements. In this study, the effect of mass eccentricity in the plan on the behavior of box-type (tunnel-form) concrete buildings with 5 and 10 stories is scrutinized. The performance level of these buildings under the Design Basis Earthquake (475 years return period) for different values of mass eccentricity has been determined. In the framework of reliability studies, fragility curves were extracted based on the IM-Based method. Ratio estimation of the uncoupled frequencies for the studied models is another achievement of this research. The results prove that the studied system has high seismic reliability under torsions due to the asymmetric distribution of mass in the plan. In the studied buildings, while moving the center of mass up to 20% of the plan, there was no drop in performance level in Design Basis Earthquake (DBE) and all of the models stayed in the immediate occupancy performance level.

Keywords: Tunnel-Form System, Mass Eccentricity, Torsionally Flexible Behavior, Fragility Analysis, Uncoupled Frequencies Ratio.

1. Introduction

In tunnel-form buildings, only slab and walls are used as vertical and lateral load-bearing elements, which have been concreted in each story, simultaneously. This type of structural system improves buildings' seismic behavior in terms of integration of members and their connections as well as promoting speed and quality of the construction. The reason for selecting the "box-type" term is because of the way this type of system is implemented. According to Fig. 1, metal casts of walls and slabs are in the form of hollow boxes; hence it is called a "box system"[1].

Within two earthquakes in Kocaeli (M_w=*7.4*) and Duzce (M_w=*7.2*) regions of Turkey in 1999, the resistance and efficiency of reinforced concrete buildings with shear walls, which were built using box-type techniques indicated that seismic performance of this system has been improved compared to the RC frames and dual systems (moment resisting frame with shear walls) [2]. Despite the wide-ranging usage of this system in mass production of industrial housing projects, especially in the Middle East, unfortunately, there is no specific provision about the design of such systems.

Fig. 1 Concrete casting of box-type buildings (photo taken by the authors from a project)

1.1.Past studies

Although studies on box system buildings are of great importance, it has received less attention from the scientific communities. In most of the past studies, the goal has intended to provide relationships for the estimation of the fundamental period [3-7]. In a few cases, studies have also been conducted to determine the seismic response reduction factor (R-factor) and system performance as well.

Relying Goel and Chopra and Lee *et al.* studies, it became clear that using equations proposed by codes to determine the period of box-type buildings does not lead to accurate results, which results in the unfitting estimation of seismic forces [3, 4].

Balkaya and Kalkan examined 80 box system buildings with different stories and plan dimensions [5]. They showed that torsional modes are dominant rather than translational modes in

many cases. According to the results, an expression was proposed for calculating the period of box-type buildings with less than 15 stories. Considering the complexity and limited usage of the former expression, Balkaya and Kalkan proposed a new equation independent of direction, to estimate the main period of such buildings. It must be noted that in this study, the torsional mode was a dominant mode of vibration in many examined models [6].

Tavafoghi and Eshghi led studies on several tunnel-form buildings with various plans and elevations. In these studies, it was made clear that the main period in each direction depends directly on the overall height of the building, and the ratio of the lateral dimensions of the building and the percentage of walls (ratio of shear walls area to total floor area) do not have considerable impact. Also, the order of the first three vibrational modes of buildings was proved to be independent of the overall height and the percentage of walls in the plan [7].

Balkaya and Kalkan carried out a pushover analysis on 2- and 5-storey tunnel-form buildings with the same plan and accordingly, the 3D membrane action was found to be a dominant force mechanism for the tunnel-form buildings. In conclusion, they proposed to utilize the response modification factor (R-Factor) of 5 and 4 for the shorter and taller buildings, respectively [2].

To examine the three-dimensional behavior of transverse walls, certain experiments were done by Kalkan and Yuksel on samples with the minimum reinforcement. Considering the low percentage of longitudinal reinforcements, the damage mode of those samples was reported to be a brittle one [8]. They performed analyses with different longitudinal reinforcement percentages and demonstrated that adding concentrated longitudinal reinforcement to the corners of walls has a positive effect on the system behavior and could change the damage mode to a more flexible one, even in low reinforcement configuration [9].

By employing the methodology prescribed by ATC-63, Tavafoghi and Eshghi conducted an analytical evaluation to calculate the response modification factor for tunnel-form structural systems and discovered that the factor equal to four could be a suitable choice [10].

According to Beheshti-Aval *et al.* studies, under the excitation of the near-fault ground motions with forwarding directivity, the pulse has a significant effect on the failure modes of the tunnel-form systems [11].

Mohsenian *et al.* explored the seismic sensitivity of the tunnel-form system to the accidental eccentricities of mass and stiffness, as well as the various configurations of centers of mass and rigidity. As they have stated, system responses are more dependent on the eccentricity of mass [12].

Mohsenian and Mortezaei assessed the effects of torsion caused by mass accidental eccentricity and observed that eccentricity by 10% of the plan dimension did not affect the reliability of these structures [13]. In this study no special pattern is considered for the mass center eccentricity and the mass moment is increase while displacing the mass center.

In another study, Mortezaei and Mohsenian employed a novel approach to investigate the effect of accidental torsion on the seismic reliability of tunnel-form buildings. Here it was found that the worst arrangement occurred when the centers of mass and rigidity are displaced in the same direction, and the center of strength is displaced in the opposite direction [14].

Through several numerical analyses, Mohsenian and Mortezaei found the RC coupling beams as the vulnerable elements of the tunnel-form buildings and proposed to use the replaceable steel multi-parted beams [15].

Mohsenian *et al.* analyzed tunnel-form buildings located in areas with high seismic hazards, whereby the flexibility of bed soil appeared to cause unexpected damage modes. Considering the high probability of overturning and sliding before the failure of the main lateral load-carrying components of the system, special attention was directed to bed soil conditions, seismicity of the

site, and choice of the foundation type [16].

In another study, Mohsenian and Mortezaei presented a new index based on maximum inter-story drift by considering both general and local failure criteria to determine the extent of damage, also, to estimate the performance level of the system under particular earthquake intensity. As a result, it was concluded that most of the proposed damage and performance levels introduced in the existing seismic codes for tunnel-form structures were indeed inefficient [17].

Mohsenian et al. [18, 19] investigated the effects of irregularities in the plan and height on the seismic reliability of tunnel-form concrete structure and proved that the requirement if geometric regularity for the tunnel-from structures is conservative.

Mohsenian and Nikkhoo scrutinized the effect of vertical mass irregularity on seismic responses of the tunnel-form structural system. Their results indicated this type of irregularity does not affect the order of mode shapes and seismic reliability of the system under DBE and MCE hazard levels [20].

A review of technical literature and previous researches on this system indicates that experimental and numerical studies have not been focused on examining the effect of mass irregularities in the plan on the seismic behavior of tunnel-form buildings. Therefore, the present work aims to address this issue.

1.2.Problem statement and research significance

In the existing analysis and design regulations, the tunnel-form system has not been considered as an independent structural system. At the moment, this new system is considered as a subset of the system of reinforced concrete load-bearing walls. However, the apparent behavioral differences between these two systems are not far from reality.

Due to the lack of sufficient information and experience on the seismic behavior of such structural system in the existing technical documents, it is evident that the measurement and identification of the factors influencing its responses based on numerically reasonable results will be very useful and considerable in the process of codification a seismic design regulation.

In many cases, despite the plan and height regularity as well as complete symmetry in the layout of the walls, the first vibrational mode of box-type buildings was reported to be torsional. Executive considerations and the necessity of removing the casts lead to the absence of structural walls in a major part of peripheral sides. This configuration results in more lateral stiffness than torsional stiffness [5, 6]. Dominant torsional behavior in the first mode is one of the important features of torsionally flexible buildings, in which, the ratio of torsional mode frequency to translational mode frequency is always smaller than one. Such buildings are more sensitive to mass eccentricity and seismic excitation [21, 22].

While constructing a building with this system, the error occurrence probability in the dimensions (length, height, and thickness) of the elements is very limited and almost impossible (the length of the casts and their distance are constant). Accordingly, changing the location of the center of rigidity in the plan is an unexpected state. It seems that mass eccentricity is the most probable type of irregularity during the operation of this type of buildings. In view of the explanation given about the effect of the eccentricity of mass on the force and displacement responses in torsionally flexible systems, it raises concerns about the new tunnel-form system.

Accordingly, the present study aims to evaluate seismic sensitivity of tunnel-form concrete system to the in-plan eccentricity of mass. For this purpose, the locations of the story mass centers are considered as variables and reliability analysis are performed to investigate the effects of accidental twists due to asymmetric distribution of mass in the plan. In the cases that torsional and

translational components simultaneously exist in the governing modes of the structure, it is impossible to determine share of each component using eigen value analysis. Therefore, the ratio of the uncoupled frequencies is used to determine the torsional behavior of structures.

This paper is organized in 6 section. The second section presents the process of early design of studied structure and the adopted assumptions in their nonlinear modeling. The details of including mass eccentricity in the plan, results of the eigen value and nonlinear static analysis are presented and discussed in section 3. The fourth section is dedicated to the fragility analysis, and in addition to presenting the development process of fragility curves, the attained results are compared with the other analysis methods. In the section 5, the parameter of uncoupled frequency ratio is extracted and a discussion on the influence of ass center eccentricity on this parameter is presented. Finally, the last section is dedicated to the conclusions.

2. Methodology

2.1. Properties of the modeled frame structures

The plan configuration of the models is given in Fig. 2. According to Fig. 2, the selected plan is regular and geometrically symmetric in both main directions. Dashed lines in the plan indicate spandrels above openings; their length and height are 1 and 0.7 meters, respectively.

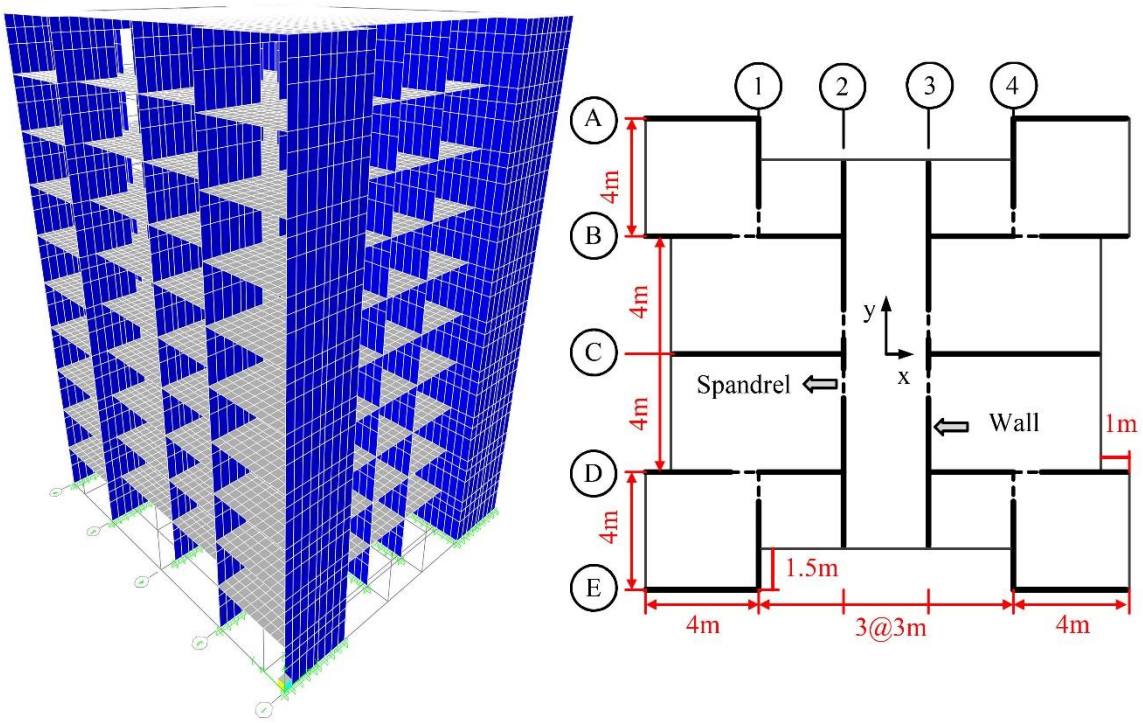

Fig. 2 Selected plan of box-type buildings and 3D-view of the 10-story building

To examine the effect of building height, models with 5 and 10 stories are considered in a region with very high seismicity hazard. The building stories are three meters in height and the subsoil has been assumed as type "II" (375 m/s $\leq \bar{V}_{s\,30} \leq$ 750 m/s, where $\bar{V}_{s\,30}$ is the average shear wave velocity in 30 meters depth) based on the Iranian Code of Practice for Seismic Resistant Design of Buildings (Standard No. 2800 [23] which is consistent with ASCE 07[24]). The selected buildings are initially designed based on ACI 318 [25] assuming no mass eccentricity (original

model); providing all design requirements (Minimum wall are equal to 3% of the plan area and walls in one direction which are at least equal to 80% of the direction walls) [26]. It must be noted that the force reduction factor for the primary design of buildings is selected 5 based on a usual value which is used by designers [15] As mentioned previously, currently, the tunnel-from concrete system is considered as a sub-system of the reinforced concrete wall systems [26] and the seismic design parameters are selected accordingly [23, 24].

As illustrated in Fig. 3, the thickness of the walls (t) is 20cm, and ϕ8 reinforcing bars with a spacing of 20cm in both vertical and horizontal directions are applied in two layers (ΦH and ΦV) (only vertical bars were used in the walls of the first four stories of the taller buildings which were ϕ12). It is evident that the requirement of minimum wall percentage in the plan controls thickness of the walls and the minimum design reinforcements are higher the required values. To provide sufficient ductility and shear strength, aside from the stirrups (Φ_D), the coupling beams were reinforced by the diagonal bars (Φ_A) [27].

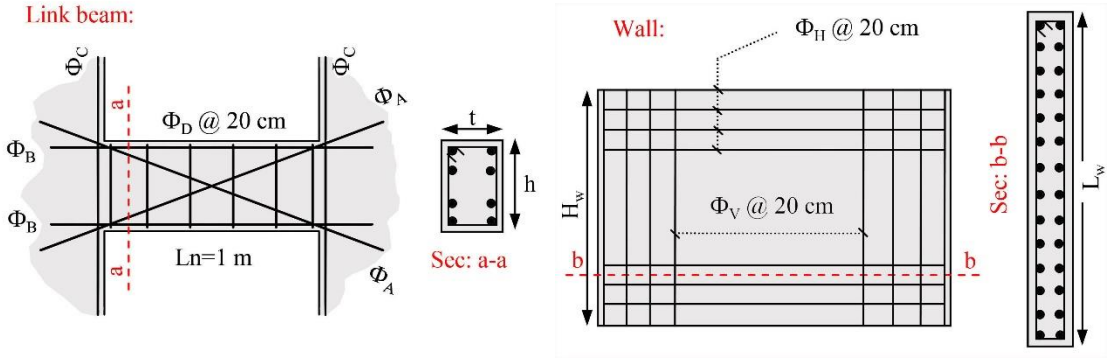

Fig. 3 An Example of Detailing for the Wall and Link Beam (Spandrel) Elements

Slab thickness is 15 cm, concrete compressive and reinforcement yield strength are assumed 25 and 400 MPa, correspondingly.

Nonlinear modeling and analyzing the selected buildings are done using PERFORM-3D (CSI 2016) software [28]. As shown in Fig. 4(a), except for a limited number of walls which have been considered as moment-control (1 m walls along the axes 2 and 3), nonlinear shear behavior is defined for all other walls and spandrels [29].The other necessary parameters for the nonlinear modeling are determined based on the generalized load-deformation curve for concrete members proposed by ASCE 41 [30] (See Fig. 4b).

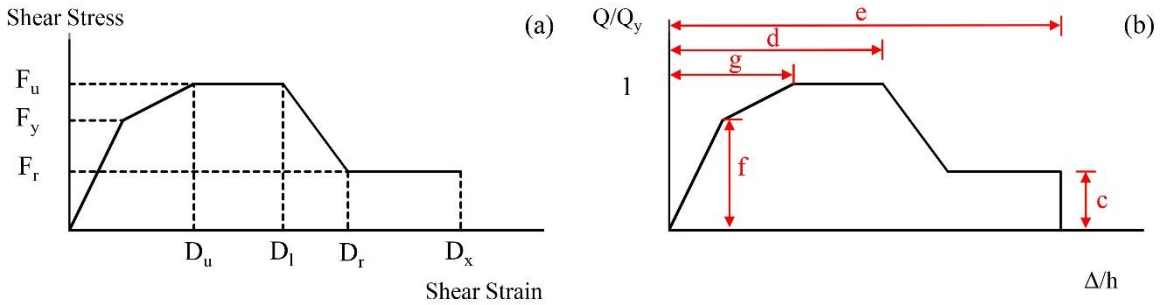

Fig. 4 (a) Nonlinear shear behavior defined in the software (b) Idealized Load-Displacement Curve for the Concrete Elements [30]

Criteria that are used for defining ductility of building elements differ depending on their behavior. As depicted in Fig. 5, for shear control walls and spandrels that are governed by shear failure, lateral drift (θ) and chord rotation (γ) are selected as the criteria [30]. In this study, for nonlinear modeling of elements with shear behavior, the nominal shear strength of the element section has been considered as ultimate strength based on ASCE41 [30].

It must be noted that for estimating the nominal shear strength of spandrels, relationships corresponding to deep beams have been used. Walls and spandrels are modeled using the "shear wall" element in the software (PERFORM-3D [28]). Other main assumptions include a) elastic out of plane behavior for walls, b) rigid diaphragm for slabs, c) rigid connections for walls base, and d) perfect bond between concrete and reinforcement.

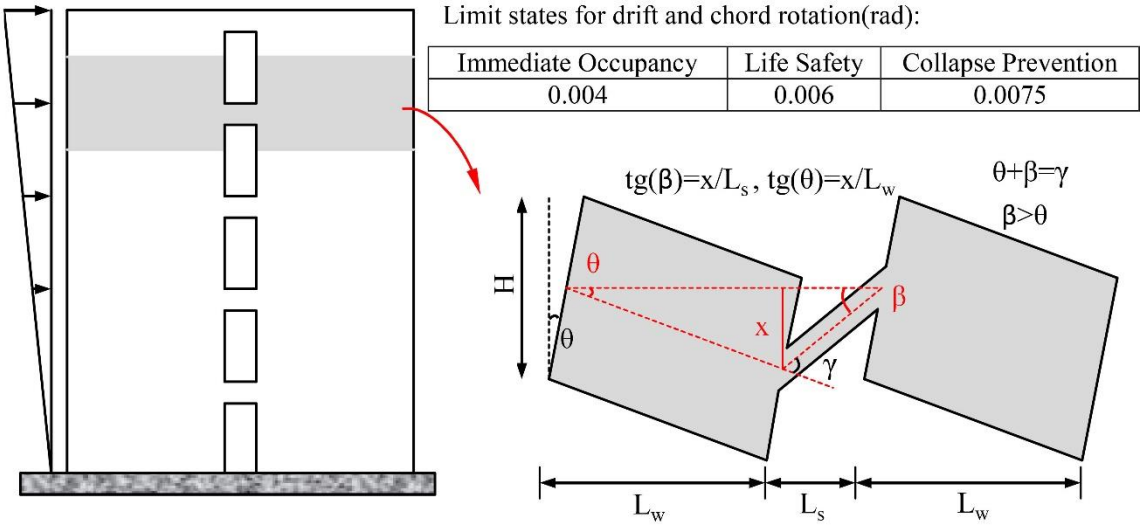

Fig. 5 Relative displacements and shear deformation in the symmetric shear walls and link beams, respectively (schematic)

3. Nonlinear analyses

By examining the percentage of walls in the plan, it is made clear that the stiffness and strength of buildings in the "*x*" direction are greater than that of in the "*y*" direction. Hence, the behavior of selected buildings has been examined only in the "*y*" direction of the plan.

According to Fig. 6, in the original model, to shift mass center along the longitudinal direction, the left side mass of the plan is increased while the right side mass of the plan is decreased in such a way that the total mass (M) of each story remains constant (the seismic mass of the roof and stories is equal to 255.44 and 330.48 ton, respectively) [14].

Having the mass inertia of the heavy and light portions of the plan (I_{M1}, I_{M2}), the story mass inertia (I_M) is derived from the transformation rule according to Eq. 1 [31]. For the studied structures and considering different values of the mass center eccentricity, the value of the mass inertia of the stories is calculate as presented in Table 1.

$$I_M = [I_{M1} + M_1(a_1)^2] + [I_{M2} + M_2(a_2)^2] \quad (1)$$

In Eq. 1, the parameters M, M_1, and M_2 are the seismic mass, and mass of the heavier and lighter portion of the plan, respectively ($M=M_1+M_2$). The parameters a_1 and a_2 are the distance between

the mass center of the heavy and light portion of the plan with the story mass center, respectively.

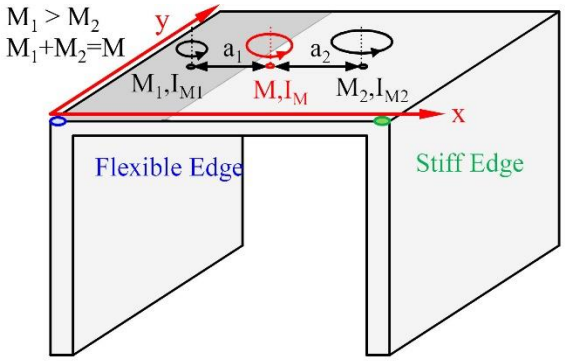

Fig. 6 Displacement of mass center (Schematic)

Dead and live loads applied to the models are the same as values considered for the primary design stage of buildings. The upper bound of gravity load effects has been assumed according to Eq. (2) in load combination.

$$Q_G = 1.1\left[Q_D + Q_L\right] \tag{2}$$

Where Q_D denotes the dead load and Q_L is the effective live load.

During all analyses, the option related to the consideration of secondary effects (P-Delta) has been activated in the software. The results of eigenvalue analysis show that in zero eccentricity (original model), the first mode is completely torsional, and increasing the eccentricity enlarges translational displacement in "y" direction to the torsion of buildings. With an increase in eccentricity, the level of translation increases and, up to a mass eccentricity of 10%, the period of the first mode in all buildings decreases (see Figs. 7 and 8).

Table 1 Mass rotational inertia of diaphragms

	Mass rotational inertia (10^6 $kg.m^2$)	
Eccentricity (%)	Floors	Roof
0	15.01	11.60
5	13.50	10.43
10	12.14	9.386
15	10.95	8.464
20	9.916	7.664

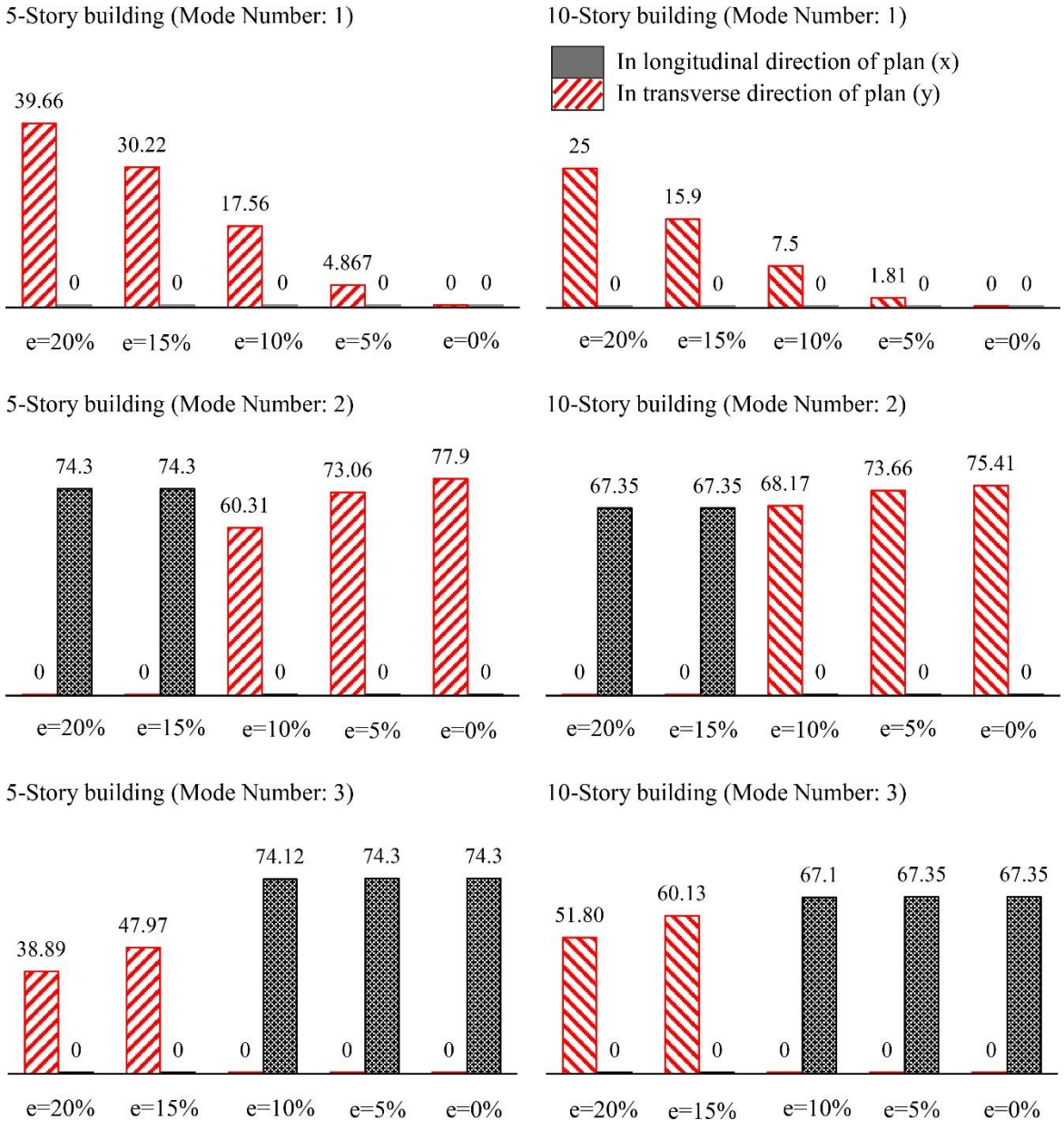

Fig. 7 Translational effective mass coefficient in the first three modes (%)

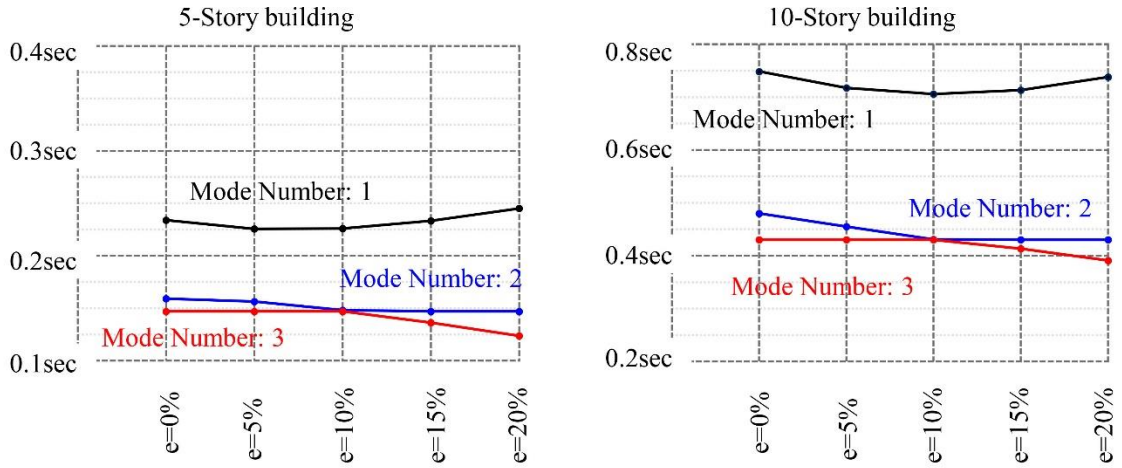

Fig. 8 Period in the first three vibrational modes

3.1. Time history analysis

Considering that selected ground motion records must conform to the site hazard, it was decided to use artificial records compatible with the design spectrum. Hence, 12 earthquake records were generated by wavelet transform based on the site demand spectrum [32]. The demand spectrum is selected from the Iranian Code of Practice for Seismic Resistant Design of Buildings (Standard No. 2800 [23]), for soil type II (375 m/s $\leq \bar{V}_{s\,30} \leq$ 750 m/s) and hazard level I (return period of 475 years and PGA=0.35g) (see Fig. 9). Peak ground acceleration in these records is close to the Design Basis Earthquake (DBE) acceleration (*PGA=0.35g*). It should be noted that for producing these records, the main component of earthquakes presented in Table 2 has been used.

For shear walls and associated components, whose inelastic behavior is controlled by shear, axial force must be less than $0.15 f_c A_g$, where A_g is the cross-section of element and f_c is the compressive strength of concrete. Otherwise, it is necessary to assume shear as a force control parameter [30]. This item has been checked for all elements. The structures with different eccentricities have been analyzed using the 12 produced artificial accelerograms, and the maximum responses have been recorded. Then, the average of the recorded responses has been considered as comparison criteria.

As it could be observed in Fig. 10, under the design basis earthquake (PGA=0.35g and 475 years return period), all elements (walls and spandrels) are at the Immediate Occupancy (IO) perf ormance level.

In the following, the maximum rotation of diaphragms and maximum drift in mass center, flexible and stiff edges has also been studied. For the sake of brevity, the results of 5- and 10-story buildings are presented and tabulated.

For all eccentricities, the high seismic demand side of the diaphragm (flexible edge), which is closer to the mass center than the low seismic demand side (stiff edge), experiences larger drifts. On the other hand, drift for both edges increases with an increase in mass eccentricity in the diaphragm. In upper stories, drifts for both edges are much larger than the drift at the mass center. These cases are more evident, especially in high-rise buildings (Fig. 11).

The average of maximum rotation of diaphragms under 12 records (Fig. 12) demonstrates that in a constant eccentricity of mass, in each building, the amount of diaphragm rotation increases along the building height. In each story, diaphragm rotation has a direct relation with the value of the mass eccentricity.

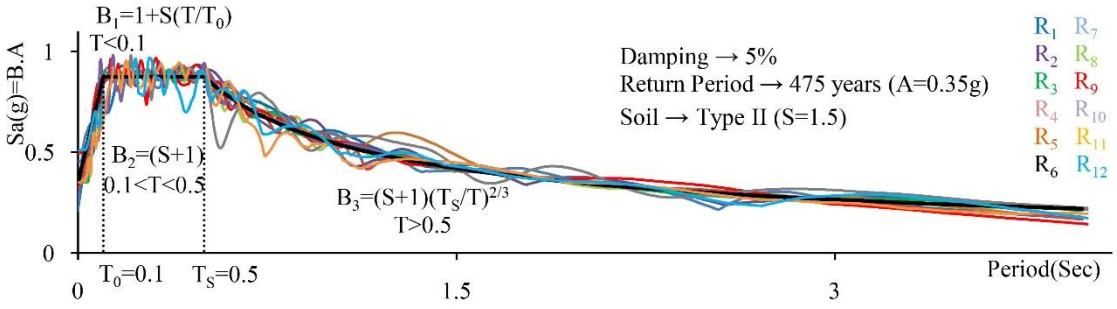

Fig. 9 Comparison of acceleration spectrum of artificial records (R_i) with the demand spectrum of the region

Table.2 The selected accelerograms for production of artificial accelerograms and IDA

Record No.	Earthquake & Year	Station	R[a](km)	Component	Mw	PGA(g)
R_1	Cape Mendocino, 1992	Eureka – Myrtle & West	41.97	90	7.1	0.18
R_2	Cape Mendocino, 1992	Fortuna – Fortuna Blvd	19.95	0	7.1	0.12
R_3	Chi Chi(Taiwan), 1999	TCU045	77.50	90	7.6	0.51
R_4	Friuli(Italy), 1976	Tolmezzo	15.82	0	6.5	0.42
R_5	Hector Mine, 1999	Hector	18.66	90	7.1	0.34
R_6	Kobe, 1995	Nishi-Akashi	16.70	0	6.9	0.51
R_7	Kocaeli (Turkey), 1999	Arcelik	53.70	0	7.5	0.22
R_8	Landers, 1992	Barstow	34.86	90	7.4	0.14
R_9	Northridge, 1994	Lake Hughes #4B - Camp Mend	31.69	90	6.7	0.06
R_{10}	Northridge, 1994	Big Tujunga, Angeles Nat F	19.74	352	6.7	0.25
R_{11}	Northridge, 1994	Hollywood – Willoughby Ave	23.07	180	6.7	0.24
R_{12}	San Fernando, 1971	Pasadena – CIT Athenaeum	25.47	90	6.6	0.11

[a] Closest Distance to Fault Rupture

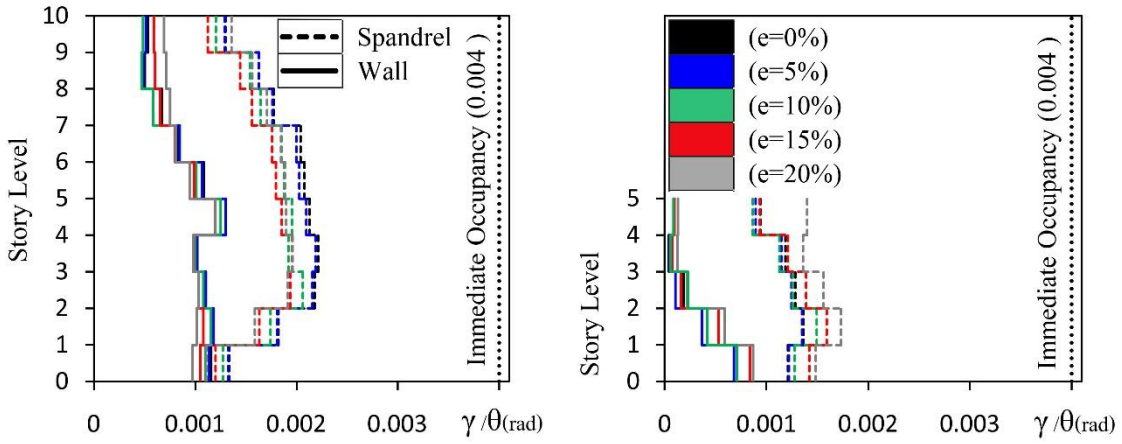

Fig. 10 Mean of maximum drift and chord rotation in walls and spandrels and limit state corresponding to immediate occupancy performance level

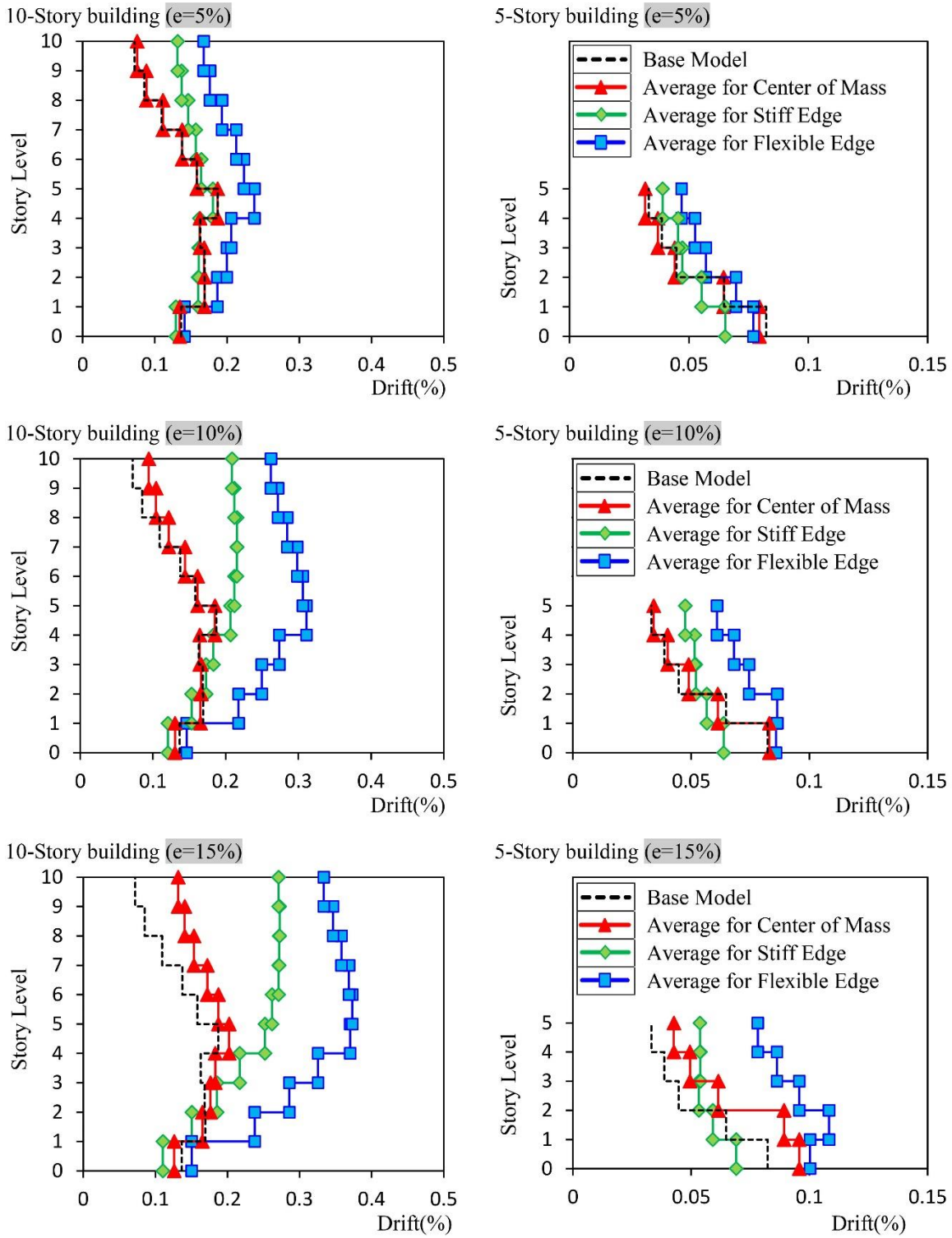

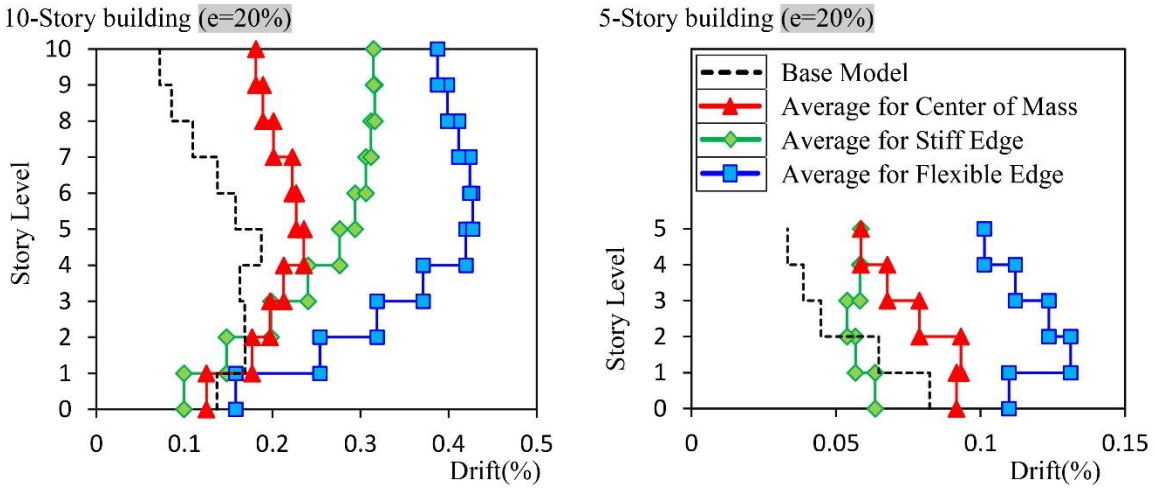

Fig. 11 Mean of maximum drifts in edges and mass center

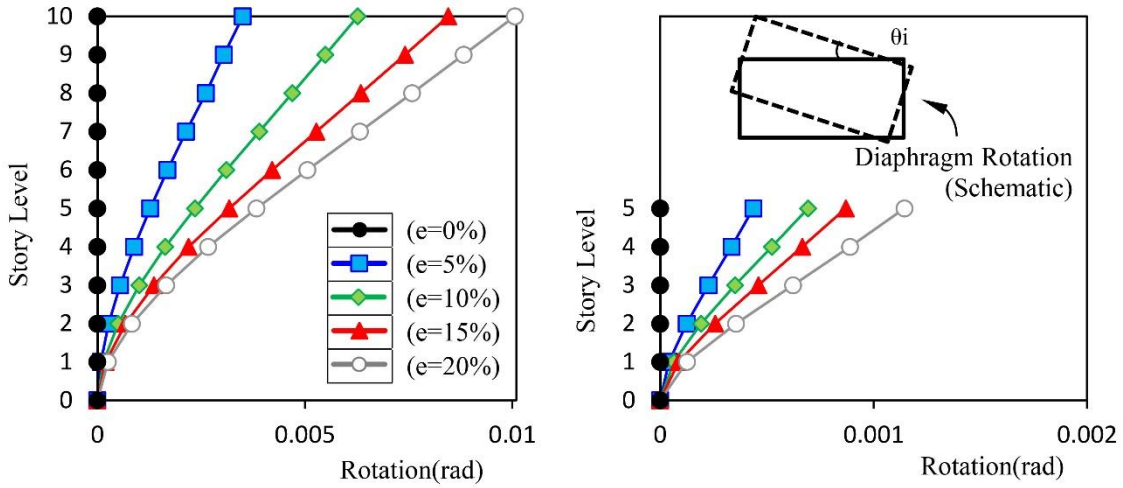

Fig. 12 Mean of maximum rotations of diaphragms

3.2. Pushover analysis

In this paper, the target displacement of buildings for pushover analysis is calculated utilizing time history analysis by averaging the maximum displacements of roof mass center under seven artificial records. Modal load distribution is assumed for nonlinear static analysis. This distribution is based on effective modes in the desired direction. The number of vibration modes is selected in such a way that at least 90% of building mass participates in the analysis.

In the following, damage in buildings is examined under the pushover analysis. In each eccentricity, the ratio of roof mass center displacement to building height is determined when the first walls (W) and spandrels (SP) reach Immediate Occupancy (IO) and Life Safety (LS) the performance levels. In Figs. 13 and 14, these ratios and ratios corresponding to the design earthquake (T.D: Target Drift) are shown on the capacity curve obtained from pushover analysis.

The results prove that mass eccentricity cause damage in walls and spandrels through which plan gets asymmetry, and elements located in axis 1 and 2 of the plan (see Fig. 2) which are closer

to mass center reach specific performance levels earlier than other elements. According to Figs 13 and 14, building capacity is greater in lower eccentricities.

In all eccentricities, for equal base shear, building walls reach life safety performance level. Spandrel beams are the most vulnerable parts of the building, but after damage, they don't have a substantial effect on the overall trend of the building capacity curve.

As long as walls do not experience damage considerably, the capacity curve does not have a severe drop; hence, one could consider the spandrels to be the secondary lateral load-bearing elements. On the other hand, under the design basis earthquake (return period of 475 years and PGA=0.35g), all walls and spandrels in the selected models have remained in the Immediate Occupancy (IO) performance level.

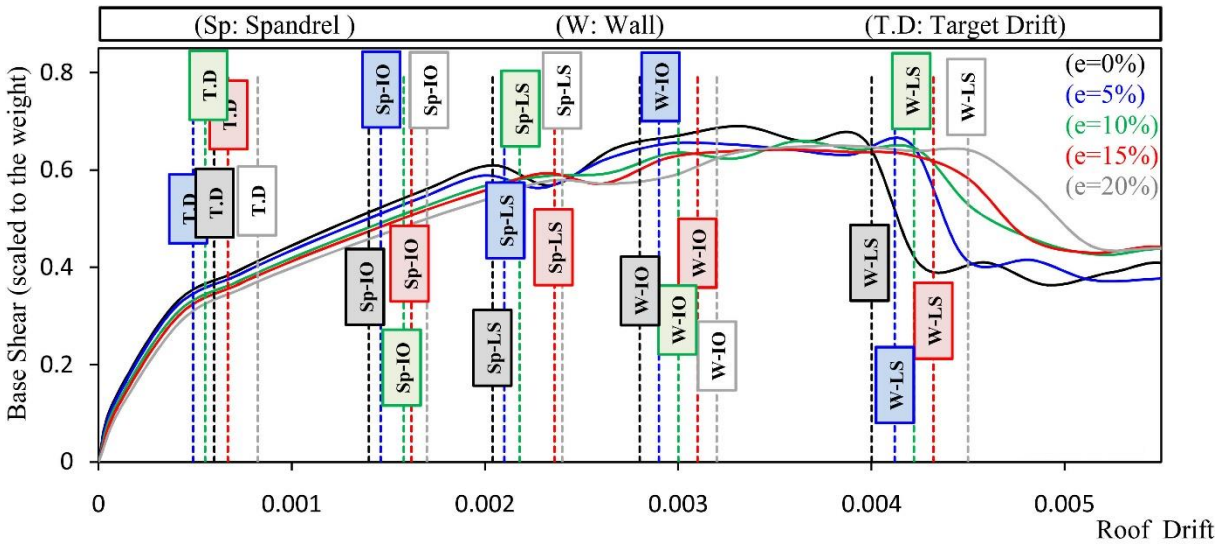

Fig. 13 Capacity curve of the 5-story building in different mass eccentricities

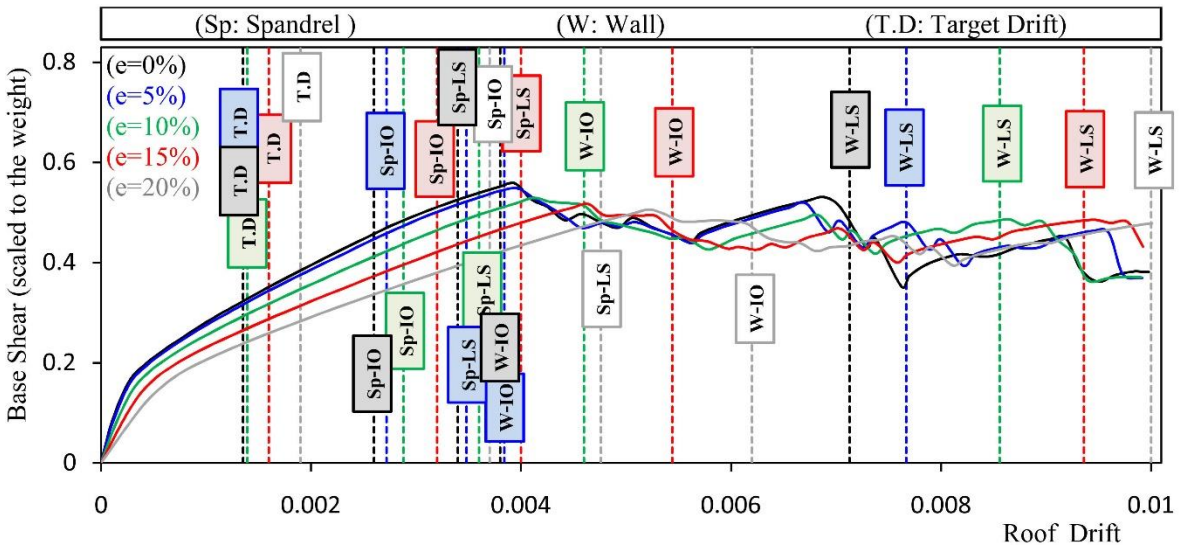

Fig. 14 Capacity curve of the 10-story building in different mass eccentricities

4. Derivation of fragility curves via Incremental Dynamic Analysis (IDA)

In Section 3, the performance levels of the structures were assessed only under the design basis earthquake using both time history and pushover analysis methods. In the time history analysis, a set of artificial accelerograms has been used in which the variation range is limited. In addition, the results of the pushover analysis depend on the pattern of lateral load distribution and, due to its static nature, this analysis method cannot provide a realistic estimate of the intensity corresponding to the different damage levels in the system. The present section is intended to compensate for these challenges, and while explaining how to extract fragility curves, the distribution functions of the structural response for different intensities of the earthquake will be presented [33]. To provide a suitable statistical population and to overcome the inherent uncertainties related to future earthquakes, the fragility curves have been extracted analytically based on the results of incremental dynamic analysis [34, 35].

If the R parameter indicates the response of the structure and LS_i designates the performance level or the limit state associated with the parameter R, IM is also one of the parameters indicating the earthquake intensity and S is the desired intensity value, then the fragility function is defined in the mathematical form given in Equation 3.

$$Fragility = P\left[R > LS_i \mid IM = S\right] \qquad (3)$$

For incremental dynamic analysis, the original earthquakes presented in Table 2 have been used. These earthquakes, according to the local soil conditions ($375\ m/s \leq Vs\ 30 \leq 750\ m/s$), are taken from the PEER website database and are classified as far-fault earthquakes [36]. After plotting the spectral response of each earthquake pair and comparing them, the principal component is determined based on the larger spectral values in the vibration frequency range of the structures and selected for analysis. Due to the correlation of translational and torsional components in the governing vibration modes of the structures, the maximum ground acceleration (PGA) is selected as the intensity measure in the incremental dynamic analysis, in order to be independent of the modal characteristics of the structure. Finally, the relative displacement and the chord rotation of the walls and link beams, respectively, are considered as the response measure (see Figure 4 again). Considering the performance levels defined in ASCE41 [30] (Figure 5), the exceedance probabilities of these limit states are determined for different intensity levels of and the corresponding fragility curves are plotted.

The probabilistic distribution of the response can be derived using two methods: constant damage level (IM-Based) and constant hazard level (EDP-Based) [37].

In the present study, a constant damage level (IM-Based) approach is considered. In order to derive the probabilistic distribution of the response in this approach, according to the schematic Figure 15, for each limit state (performance level), the peak values of the ground acceleration are taken from the curves obtained from incremental dynamic analysis. In another step, assuming the lognormal distribution for the recorded values [38], after calculating the mean parameters (μ) and the standard deviation (δ) for the obtained values, a probability density function (f (x)) is established for each limit state. By substituting a value for X_0 as an intensity level, the area under the probability density function curve from $-\infty$ to X_0 shows the probability that the structure will exceed the desired limit state at this level of intensity (P). Obviously, the difference between the collected value and 1 (1-P) results in the reliability of the desired performance level and means the possibility of noy exceeding the given performance level. Repetition of the described procedure

and extraction of probability values (P) for different intensities will lead to extraction of fragility curves for the desired performance level [39].

The general trend in the EDP-Based approach is similar, except that the probabilistic distribution curve of the structural response is presented for a constant hazard level. A value of (P) in this approach means reliability (not fragility) [16, 19].

Examination of the fragility curves in Figures 16 and 17 shows that the link beams are the first vulnerable parts of the system (probability values for these elements are higher than walls). Increasing the eccentricity of the mass slightly increases the probability of reaching the performance levels. As the height of the structure increases, the probability that the elements reaching different performance levels also increases. It is observed that the height of structure had a greater effect on the probability values than the mess center eccentricity.

The probability that the elements of the 5-story structure (including wall and ln beam) under the design basis earthquake (return period of 475 years and the peak acceleration of 0.35g) and for all values of the mass center eccentricity reach the immediate occupancy level is less than 1% and almost zero. Under the maximum probable earthquake (return period of 2475 years and the peak acceleration equal to 0.55g), this probability is less than 10% for the link beams and less than 3% for the walls.

In the 10-story building under the design earthquake, and for all values of mass center eccentricity, the probabilities that the walls and link beams reach the immediate occupancy level are less than 2 and 10%, respectively. Under the maximum probable earthquake, these probabilities are less than 15% and 30%, respectively.

In both structures and for all of the considered eccentricities, it can be said that the link beams and walls provide the immediate occupancy performance level at the design and the maximum probable hazard levels.

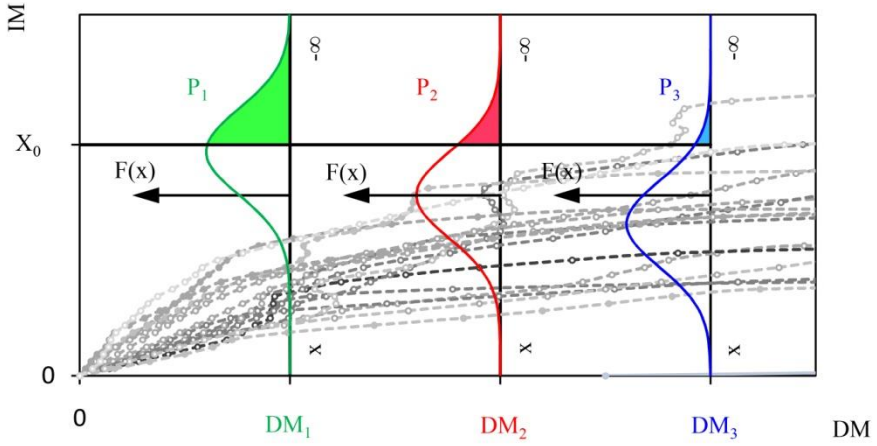

Fig. 15 Probability exceedance of a fixed performance level in an assumed hazard level

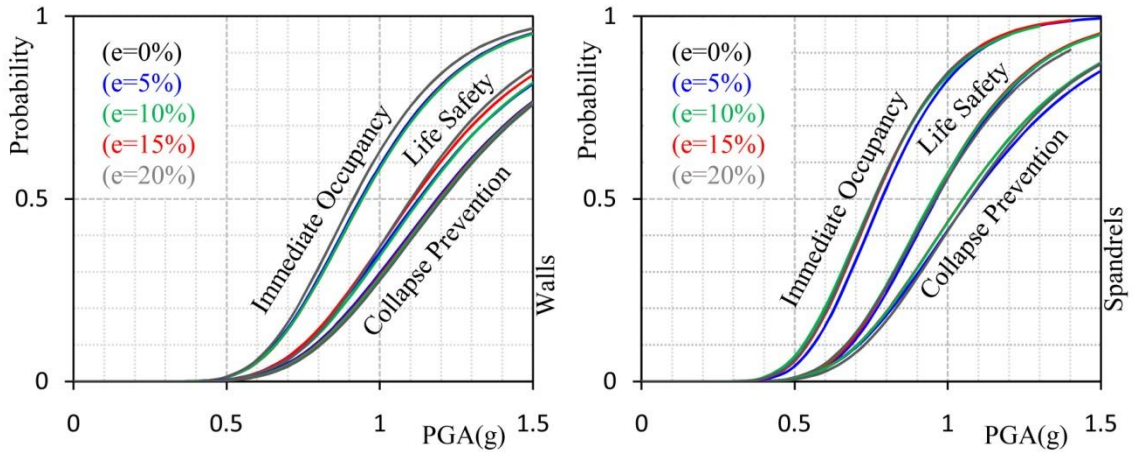

Fig. 16 Fragility curves for different performance levels in the walls and spandrels (5-story building)

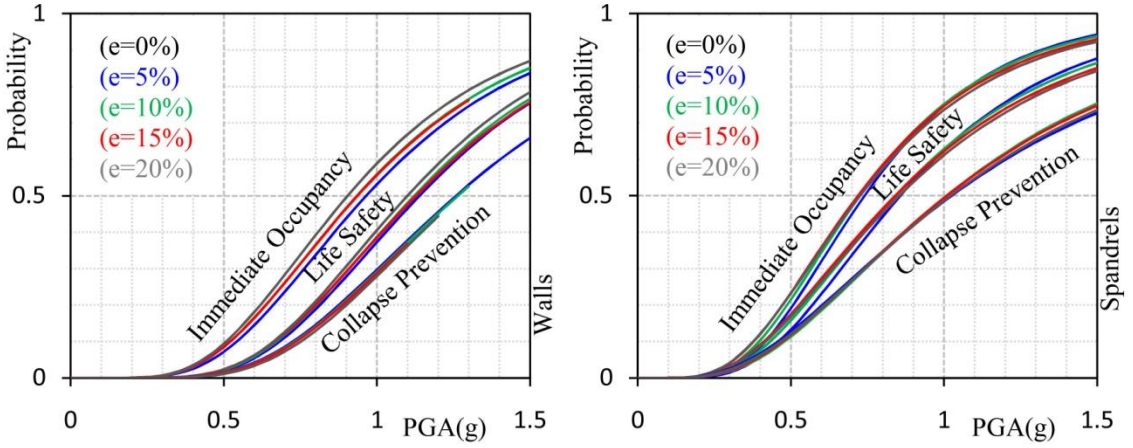

Fig. 17 Fragility curves for different performance levels in the walls and spandrels (10-story building)

5. Examining the uncoupled frequency ratio in selected buildings

Parameter Ω is a proper quantity for evaluating torsional behavior in buildings. Accordingly, the structures with $\Omega<1$ are torsional flexible, and those with $\Omega\geq1$ are considered torsional stiff [40, 41]. It is determined by dividing torsional frequency by the translational frequency, based on the following equation (Eq. (4)):

$$\Omega = \sqrt{\frac{K_\theta}{K} \times \frac{M}{I_M}} \tag{4}$$

Where K_θ is torsional stiffness, I_M is the mass rotational inertia, K is lateral stiffness, and M is the mass. Torsional stiffness and mass rotational inertia have been calculated in the stiffness and mass center, respectively [42].

$$\Omega^2 = \frac{K_{\theta,CS} \times M}{I_{M,CM} \times K} = \frac{\rho_K^2}{\rho_M^2} \tag{5}$$

In Eq. (5), ρ_k is the normalized stiffness gyration radius around the stiffness center, and ρ_m is the normalized mass gyration radius around the mass center, which are determined in the following form (Eqs. (6) and (7)):

$$\rho_k = \frac{1}{b}\sqrt{\frac{K_{\theta,CS}}{K}}\ ,\ \rho m = \frac{1}{b}\sqrt{\frac{I_{M,CM}}{M}} \qquad (6),(7)$$

In which, b is the plan width. For multi-story buildings, there is no straight forward way to calculate ρ_k. To overcome this problem, the torsional index (Δ) is used. This index is defined as the ratio of displacements of flexible edges (the edge with high seismic demand) to stiff edges (the edge with low seismic demand) of the diaphragm in a way that the building is in the elastic range and under the pushover analysis with triangular lateral load distribution pattern applying at the mass centers. Using Eq. (8), one could estimate ρ_k [43]. In this study, ρ_k has been calculated through this equation for each story.

$$\Delta = \frac{\delta_{\min}}{\delta_{\max}} = 1 - \left(\frac{e}{\rho_k^2}\right)\left(1 + \left(\frac{e}{\rho_k^2}\right)\left(0.5 + \eta\right)\right)^{-1} \qquad (8)$$

δ_{min}: Minimum displacement in edges

δ_{max}: Maximum displacement in edges

Δ: Ratio of displacements

e: Distance between the mass and stiffness centers of each story which normalized with respect to the plan width.

η: Distance between geometric center and stiffness center in stories (normalized with respect to the plan width).

By assuming that buildings are completely regular and symmetric in terms of geometry, properties of elements' cross-sections, and their location in the plan, the value of parameter (η) in Eq. (8) is considered to be zero. Quantitative values of the calculated Ω for each floor have been presented in Fig. 18.

It is clear that for all mass eccentricities, Ω is lower than 1, and buildings are torsionally flexible. With an increase in the number of stories, this parameter decreases, which shows more torsion in higher stories. In each building, it is found that with an increase in mass eccentricities, Ω increases, which indicates an increase in translation component compared to the torsion in each story. In low-rise buildings, Ω is more sensitive to the asymmetric distribution of mass. Results presented in this section are in congruence with the results obtained from the non-linear time history analysis in section (3.1) (see Fig. 11 again).

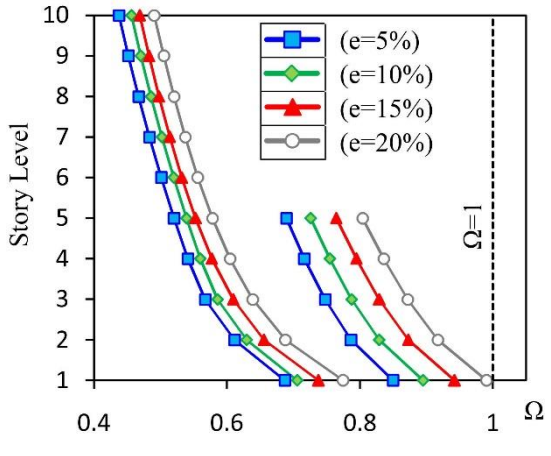

Fig. 18 Uncoupled frequencies ratio

6. Conclusions

In the selected models, results showed acceptable seismic performance of box-type buildings under the torsion due to asymmetric mass distribution in the plan. Pushover analysis demonstrated that:

The mass center eccentricity varies the damage distribution pattern in the structure, but has no effect on its performance level. Under the design basis earthquake (return period of 475 year- peak ground acceleration of 0.35g) the structural system always experiences the immediate occupancy performance level.

The probability of reaching the immediate occupancy level for the structural elements (walls and linking beams) of the five-story structure under the design basis earthquake is lower than 1% and approximately is zero. In the case of the maximum probable earthquake (return period of 2475 year and the peak ground acceleration of 0.55g), this probability is less than 10% for the linking beams and less than 3% for the walls.

For the 10-story structure under the design basis earthquake, and for all the values of eccentricity, the probability of reaching the immediate occupancy level is less than 2 and 10% for the walls and linking beams, respectively. under the maximum probable earthquake, these probabilities are 15 and 30%, respectively.

The link beams are the first elements that experience damage in the system, therefore the considerable drop in the capacity of the system occurs due to damage formation in the walls. Nevertheless, the maximum capacity of the system is not sensitive to the mass center eccentricity.

The structures demonstrate torsional flexible behavior. Although inclusion of the mass center eccentricity in the models increases share of the translational components in the response of the structures, but the diaphragm rotations in the system are considerable and therefore, drift of the story mass centers is not an appropriate measure for the structural damage.

Since the story mass centers in the models experience lower displacements in comparison with the diaphragm edges, the roof mass center is not an appropriate control point for controlling the displacement requirements, especially in taller structures.

References

[1] Mirghaderi R, Moghadam A, Yousefpour H, Pahlevan H. Assessment of nonlinear seismic behavior of tunnel form

concrete buildings. 1st International Conference on Concrete Technology; Tabriz; Iran; 6-7 November 2009.

[2] Balkaya C, Kalkan E. Seismic Vulnerability, Behavior and Design of Tunnel Form Building Structures. Engineering Structures 2004, 26(14): 2081-2099.

[3] Goel RK, Chopra AK. Period Formulas for Concrete Shear Wall Buildings. Journal of Structural Engineering 1998; 124(4): 426-433.

[4] Lee LH, Chang KK, Chun YS. Experimental Formula for the Fundamental Period of RC Building with Shear Wall Dominant Systems. The Structural Design of Tall Buildings 2000, 9(4): 295-307.

[5] Balkaya C, Kalkan E. Estimation of Fundamental Periods of Shear-Wall Dominant Building Structures, Earthquake Engineering and Structural Dynamics 2003; 32(7): 985-998.

[6] Balkaya C, Kalkan E. Relevance of R-factor and Fundamental Period for Seismic Design of Tunnel-Form Building. 13th World Conference on Earthquake Engineering, Vancouver, Canada, 2004.

[7] Tavafoghi A, Eshghi S. Seismic Behavior of Tunnel Form Concrete Building Structures", The 14th World Conference on Earthquake Engineering, Beijing, China, 12-17 October, 2008.

[8] Kalkan E, Yuksel SB. Pros and Cons of Multi-Story RC Tunnel-Form (Box-Type) Buildings. The Structural Design of Tall and Special Buildings 2007, 17(3): 601-617.

[9] Yuksel SB, Kalkan E. Behavior of Tunnel Form Buildings Under Quasi-Static Cyclic Lateral Loading. Structural Engineering and Mechanics 2007; 27(1): 99-115.

[10] Tavafoghi A, Eshghi S. Evaluation of Behavior Factor of Tunnel-Form Concrete Building Structures Using Applied Technology Council 63. The Structural Design of Tall and Special Buildings 2011, 22(8): 615-634.

[11] Beheshti-Aval SB, Mohsenian V, Sadegh Kouhestani H. Seismic performance-based assessment of tunnel form buildings subjected to near- and far-fault ground motions. Asian Journal of Civil Engineering 2018; 19(1): 79-92.

[12] Mohsenian V, Rostamkalaee S, S.Moghadam A. Seismic reliability of tunnel form concrete buildings subjected to accidental torsion: A case study, 16th European Conference on Earthquake Engineering, Thessaloniki, Greece 2018.

[13] Mohsenian V, Mortezaei A. Seismic reliability evaluation of tunnel form (box-type) RC structures under the accidental torsion. Structural Concrete 2018; 1-12.

[14] Mortezaei A, Mohsenian V. Reliability-Based Seismic Assessment of Multi-Story Box System Buildings under the Accidental Torsion, Journal of Earthquake Engineering 2019; DOI:10.1080/13632469.2019.1692738.

[15] Mohsenian V, Mortezaei A. Effect of steel coupling beam on the seismic reliability and R-factor of box-type buildings. Structures and Buildings 2019, 172(10): 721-738.

[16] Mohsenian V, Nikkhoo A, Hejazi F. An investigation into the effect of soil-foundation interaction on the seismic performance of tunnel-form buildings, Soil Dynamics and Earthquake Engineering 2019; 125, https://doi.org/10.1016/j.soildyn.2019.105747.

[17] Mohsenian V, Mortezaei A. New proposed drift limit states for box-type structural systems considering local and global damage indices. Advances in Structural Engineering 2019; 22(15): 3352-3366.

[18] Mohsenian V, Nikkhoo A, Hajirasouliha I. Estimation of seismic response parameters and capacity of irregular tunnel-form buildings. Bulletin of Earthquake Engineering 2019; 17(9): 5217-5239.

[19] Mohsenian V, Hajirasouliha I, Mariani S, Nikkhoo A. Seismic reliability assessment of RC tunnel-form structures with geometric irregularities using a combined system approach. Soil Dynamics and Earthquake Engineering 2020; https://doi.org/10.1016/j.soildyn.2020.106356.

[20] Mohsenian V, Nikkhoo A. A study on the effects of vertical mass irregularity on seismic performance of tunnel-form structural system. Advances in Concrete Construction 2019, **7**(3): 131-141.

[21] De Stefani M. Pintucchi B. A review of research on seismic behaviour of irregular building structures since 2002. Bulletin of Earthquake Engineering 2008; 6(2): 285-308.

[22] Seyedtaghia SA, Moghadam AS. Efficiency of Standard 2800 Provisions for Buildings with Low Torsional to Translational Modal Frequencies Ratio. Steel and Structure 2009; 5(5): 40-51.

[23] Permanent Committee for Revising the Standard 2800 (2014), Iranian code of practice for seismic resistant design of buildings, 4th edition, Building and Housing Research Center, Tehran, Iran.

[24] ASCE (2010), Minimum Design Loads and Associated Criteria for Buildings and Other Structures, ASCE/SEI 7-10, American Society of Civil Engineers, Reston, Virginia.

[25] ACI 318 (2014), Building code requirements for structural concrete and commentary, American Concrete Institute; Farmington Hills, MI, USA.

[26] BHRC (2007), A step in direction of building industrialization. First Edition, Building and Housing Research Center Press, pages 21 and 22 [In Persian].

[27] Paulay T, Binney JR. Diagonally Reinforced Coupling Beams of Shear Walls. Shear in reinforced concrete. ACI Special Publications 1974; 42: 579-598.

[28] Computers and Structures Inc (CSI) (2016), Structural and Earthquake Engineering Software, PERFORM-3D Nonlinear Analysis and Performance Assessment for 3-D Structures, Version 6.0.0, Berkeley, CA, USA.

[29] Allouzi R, Alkloub A. New nonlinear dynamic response model of squat/-slender flanged/non-flanged reinforced concrete walls. Structural concrete 2017; 1-15. https://doi.org/10.1002/suco.201700066.

[30] ASCE/SEI41-17 (2017), Seismic evaluation and retrofit of existing buildings, American Society of Civil Engineers.

[31] Beer F, Johnston Jr. E. Vector Mechanics for Engineering; Vol 1, Statics, 3rd SI Metric Edition, 1996.

[32] Hancock J, Watson-Lamprey J, Abrahamson NA, Bommer JJ, Markatis A, McCoy E, Mendis R. An improved method of matching response spectra of recorded earthquake ground motion using wavelets. Journal of Earthquake Engineering 2006; 10: 67-89.

[33] Cimellaro GP, Reinhorn AM, Bruneau M, Rutenberg A. Multi-Dimensional Fragility of Structures: Formulation and Evaluation. Multidisciplinary Center for Earthquake Engineering Research 2006; MCEER-06-0002.

[34] Bulleit WM. Uncertainty in Structural Engineering. Practice Periodical on Structural Design and Construction 2008; 13(1): 24-30.

[35] Vamvatsikos D, Cornell CA. Incremental Dynamic Analysis. Earthquake Engineering and Structural Dynamics 2002; 31 (3), 491-514.

[36] PEER Ground Motion Database, Pacific Earthquake Engineering Research Center, Web Site: http://peer.berkeley.edu/peer-ground-motion-database; Accessed: Jan 2019.

[37] Zareian F, Krawinkler H, Ibbara I, Lignos D. Basic concepts and performance measures in prediction of collaps e of buildings under earthquake ground motions. The Structural Design of Tall and Special Buildings 2010; 19(6): 16 7-181.

[38] Baker JW, Cornell CA. A vector valued ground motion intensity measure consisting of spectral acceleration and epsilon. Earthquake Engineering and Structural Dynamics 2005; 34:1193-1217.

[39] Mohsenian V, Filizadeh R, Ozdemir Z, Hajirasouliha I. Seismic performance evaluation of deficient steel moment-resisting frames retrofitted by vertical link elements. Structures 2020; 26: 724–736.

[40] Humar J, Yavari S, Saatcioglu M. Design for forces induced by seismic torsion. Canadian Journal of Civil Engineering 2003; 30(2): 328-337.

[41] Haj Seiyed Taghia SA, Moghadam AS, Ghafory Ashtiany M. Seismic performance of torsionally stiff and flexible multi-story concentrically steel braced buildings. The Structural Design of Tall and Special Buildings 2012; 23(2), DOI: 10.1002/tal.1031.

[42] Annigeri S, Mittal AK. Uncoupled Frequency Ratio in Asymmetric Buildings", Earthquake Engineering and Structural Dynamics 1996; 25(8):871-881.

[43] Tso WK, Wong CM. Euro Code 8 Seismic Torsional Provision Evaluation. European Earthquake Engineering 1995, *IX*; 9(1): 23-33.